$\alpha_4\beta_7$ independent pathway for CD8$^+$ T cell–mediated intestinal immunity to rotavirus

Nelly A. Kuklin,[1] Lusijah Rott,[2] Jama Darling,[1] James J. Campbell,[3,4] Manuel Franco,[1] Ningguo Feng,[1] Werner Müller,[5] Norbert Wagner,[6] John Altman,[7] Eugene C. Butcher,[2,8] and Harry B. Greenberg[1,8]

[1]Department of Microbiology and Immunology,
[2]Department of Pathology, Stanford University School of Medicine, Stanford, California, USA
[3]Children's Hospital, Joint Program in Transfusion Medicine, Boston, Massachusetts, USA
[4]Department of Pathology, Harvard Medical School, Boston, Massachusetts, USA
[5]Department of Pediatrics, University of Bonn, Bonn, Germany
[6]Institute of Genetics, University of Cologne, Cologne, Germany
[7]Emory Vaccine Center and Department of Microbiology and Immunology, Emory University School of Medicine, Atlanta, Georgia, USA
[8]Veterans Affairs Palo Alto Health Care System, Palo Alto, California, USA

Address correspondence to: Nelly A. Kuklin, WP16-214C PO Box 4, Merck Research Laboratories, West Point, Pennsylvania 19486, USA. Phone: (215) 652-4893; Fax: (215) 652-7320; E-mail: nelly_kuklin@merck.com.

Received for publication August 2, 2000, and accepted in revised form November 6, 2000.

Rotavirus (RV), which replicates exclusively in cells of the small intestine, is the most important cause of severe diarrhea in young children worldwide. Using a mouse model, we show that expression of the intestinal homing integrin $\alpha_4\beta_7$ is not essential for CD8$^+$ T cells to migrate to the intestine or provide immunity to RV. Mice deficient in β7 expression ($\beta7^{-/-}$) and unable to express $\alpha_4\beta_7$ integrin were found to clear RV as quickly as wild-type (wt) animals. Depletion of CD8$^+$ T cells in $\beta7^{-/-}$ animals prolonged viral shedding, and transfer of immune $\beta7^{-/-}$ CD8$^+$ T cells into chronically infected Rag-2–deficient mice resolved RV infection as efficiently as wt CD8$^+$ T cells. Paradoxically, $\alpha_4\beta_7^{hi}$ memory CD8$^+$ T cells purified from wt mice that had been orally immunized cleared RV more efficiently than $\alpha_4\beta_7^{low}$ CD8$^+$ T cells. We explained this apparent contradiction by demonstrating that expression of $\alpha_4\beta_7$ on effector CD8$^+$ T cells depends upon the site of initial antigen exposure: oral immunization generates RV-specific CD8$^+$ T cells primarily of an $\alpha_4\beta_7^{hi}$ phenotype, but subcutaneous immunization yields both $\alpha_4\beta_7^{hi}$ and $\alpha_4\beta_7^{low}$ immune CD8$^+$ T cells with anti-RV effector capabilities. Thus, $\alpha_4\beta_7$ facilitates normal intestinal immune trafficking to the gut, but it is not required for effective CD8$^+$ T cell immunity.

J. Clin. Invest. **106**:1541–1552 (2000).

Introduction

Mucosal immunity provides the first level of defense against foreign antigens. Some mucosal pathogens, like rotavirus (RV) in the gut and respiratory syncytial virus in the respiratory tract, replicate at the site of entry and cause disease by local tissue damage (1). In such mucosal infections, systemic memory cells are frequently unable to prevent clinical symptoms; optimal protective immunity correlates with the presence of effector cells or local antibody at mucosal sites (1, 2).

CD8$^+$ T cell responses are a major defense against viral infections at different tissue sites. The ability of lymphocytes to traffic to relevant tissues is critical for an effective immune response and is mediated by homing receptors on effector cells that have cognate ligands at peripheral or mucosal sites (3). Intestinal CD8$^+$ T cell immunity, for example, has been specifically correlated with expression of $\alpha_4\beta_7$ integrin (4). This integrin and its ligand, mucosal adressin cell adhesion molecule (MAdCAM-1) are known to play an important role in homing of activated lymphocytes to Peyer's patches and the lamina propria (5–7). Using adoptively transferred immune CD8$^+$ T cells in a murine RV (mRV) model, our earlier experiments supported the hypothesis that $\alpha_4\beta_7$ integrin expression on CD8$^+$ T cells was critical for effective intestinal immunity (8). In that study we demonstrated that $\alpha_4\beta_7^{hi}$ but not $\alpha_4\beta_7^{low}$ memory CD8$^+$ T cells from wild-type (wt) mice that had been orally immunized were able to resolve chronic infection when transferred into Rag-2 deficient mice. It was unclear however, whether the ability of $\alpha_4\beta_7^{hi}$ CD8$^+$ T cells to resolve RV infection was solely dependent upon $\alpha_4\beta_7$ expression or whether it reflected a higher frequency of anti-RV immune CD8$^+$ T cells in the $\alpha_4\beta_7^{hi}$ population generated following oral immunization with RV.

Determination of the function of β7 integrins has recently been facilitated by development of a β7 gene knockout ($\beta7^{-/-}$) mouse (9–13). These $\beta7^{-/-}$ mice, lacking both $\alpha_4\beta_7$ and $\alpha_E\beta_7$ integrins, have dramatically reduced numbers of intestinal lymphocytes (9). Whereas $\alpha_4\beta_7$ integrin has been implicated in lymphocyte homing to the intestine, $\alpha_E\beta_7$ integrin is believed to retain CD8$^+$ T

cells in the intraepithelial compartment of the intestine (14). Taking advantage of the existence of $\beta7^{-/-}$ mice, we set out to investigate the functional properties of $CD8^+$ T cells lacking $\alpha_4\beta_7$ expression, using an RV intestinal infection model. We specifically sought to determine whether such cells could localize at the site of RV infection and efficiently participate in antiviral immunity.

Methods

Viruses. Stocks of wt mouse RV (EC) were prepared as intestinal homogenates, and the titer (Diarrhea Dose 50 [DD_{50}]) was determined by infecting suckling mice as previously described (15). Tissue culture–adapted rhesus RV (RRV) was prepared as described (16). RRV inactivation was performed as previously described by Groene and Shaw (17). Briefly, psoralen 4′-aminomethyl1-4, 5′ 8-trimethylpsoralenhydrochloride (HRI Associates, San Diego, California, USA) at a concentration of 40 μg/ml was added to 1 ml of purified RRV (titer of 5×10^9 focus-forming units per ml) and the virus was ultraviolet (UV) inactivated for 40 minutes using UV light (George W. Gates & Co., Franklin Square, New York, USA). The lack of viral infectivity following inactivation was confirmed by virus focus assay (18).

Mice. C57BL/6 mice were obtained from Charles River Laboratory (Hollister, California, USA). β_7 knockout ($\beta7^{-/-}$) mice (C57BL/6 background) were produced by Norbert Wagner (Institute for Genetics, University of Cologne) as previously described (9). Rag-2–deficient (Rag-2) mice were obtained from Taconic Laboratories (Germantown, New York, USA). Th1.1 mice were obtained from Jackson Laboratories (Bar Harbor, Maine, USA). All mice were bred in the Palo Alto Veteran Administration vivarium. Mice were routinely tested for RV antibodies (or RV shedding for Rag-2 mice) prior to infection and tested negative.

Virus inoculation. Oral immunizations were performed as follows. Three- to five-week-old $\beta7^{-/-}$, Rag-2, and C56BL/6 mice were orally gavaged (using a feeding needle) with 5×10^5 DD_{50} of mRV strain EC after receiving 100 μl of 1.33% sodium bicarbonate to neutralize stomach acid. Rag-2 mice (used as recipients for adoptive transfer) were infected 1–4 months prior to use in the cell transfer studies. Stools were collected 2 weeks after viral inoculation of Rag-2 mice to confirm the establishment of chronic infection. Systemic immunizations were performed on 4- to 5-week-old C57BL/6 mice. The mice were injected subcutaneously with 20 μg of inactivated RRV with CFA (Sigma Immuno-Chemicals, St. Louis, Missouri, USA). Fifteen days later the same animals were injected subcutaneously a second time with 20 μg/mouse of inactivated RRV in Incomplete Freund's Adjuvant (IFA) (Sigma Immuno-Chemicals).

Detection of RV antigen. For detection of RV antigen (Ag), sandwich ELISA was carried out as described previously (15).

Detection of anti-RV antibodies. Virus-specific antibodies were detected using standard ELISA. Plates were first coated as described above and then incubated overnight at 4°C with 1:5 dilution of RRV stock. After washing, 10% stool suspensions were added to the plates and incubated overnight at 4°C as described above. Antibody was detected with horse radish peroxidase–conjugated (HRP-conjugated) anti-mouse IgA or IgG (Kirkegaard & Perry Laboratories Inc., Gaithersburg, Maryland, USA). Stools from noninfected animals were used as negative controls. The concentration of anti-RV antibodies was determined by running an IgA standard in each individual plate as described previously (19). Briefly, three rows per plate were coated with purified goat anti-mouse IgA (Kirkegaard & Perry Laboratories Inc.) followed by blocking with 5% dry nonfat milk and washing with $Tween_{20}$. A standard of 250 ng/ml of purified mouse IgA isotype (PharMingen, San Diego, California, USA) was serially diluted and added to the plate. The antibodies were detected using anti-mouse IgA conjugated to HRP as described above. Absorbance at 405 nm was measured to provide standard curve.

$CD8^+$ T-cell purification, FACS sorting, and adoptive transfer experiments. RV immune $\beta7^{-/-}$ or wt mice were used as donors for adoptive transfer of $CD8^+$ T cells into chronically infected Rag-2 mice. Thirty days following oral infection with mRV EC, spleens from the donor mice were harvested, and cell suspensions were made using a sterile cell strainer (40 μm) (Fisher Scientific, Springfield, New Jersey USA). The splenocytes were washed with Dulbecco's modified Eagle's medium supplemented with 10% FBS (DMEM-10) and the red blood cells were lysed using lysing buffer (8.3 g/l ammonium chloride in 0.01 M tris-HCL buffer, pH 7.5). The cell suspensions were affinity purified through CD8 purification columns (R&D Systems Inc., Minneapolis, Minnesota, USA) ($1–2 \times 10^8$ cells per column). The purity of the cells was generally 86 ± 3%. The $CD8^+$ T cells were subsequently stained with antibodies to CD8 (Lyt2) and antibodies to T cell–receptor β chain (TCR-β chain) conjugated to FITC or phycoerythrin (PE), respectively. The cells were then sorted using a modified FACStar (Becton Dickinson Immunocytometry Systems, San Jose, California, USA) with a single 488-mm argon laser and three fluorescence detectors. To avoid possible contamination with B cells, the affinity-purified splenocytes were sorted twice. The purity after the first sort was 97–99% and after the second sort was ≥ 99.7%. Sorted cells were resuspended in sterile HBSS, and 5×10^5, 5×10^4, 5×10^3 wt, or $\beta7^{-/-}$ $CD8^+$ $TCR\alpha\beta^+$ T cells were injected intraperitoneally into chronically infected Rag-2 mice. The ability of the transferred cells to resolve chronic infection was determined by measuring RV Ag shedding in the stools of the recipients.

Experiments in which wt and $\beta7^{-/-}$ $CD8^+$ T cells were transferred simultaneously into the same recipient Rag-2 mice were also performed. To distinguish $\beta7^{-/-}$ from wt $CD8^+$ T cells, we used Thy1.1 wt mice in these experiments. Splenocytes from immune wt (Thy1.1) and $\beta7^{-/-}$ (Thy1.2) mice were affinity-purified using CD8 purifi-

cation column as described above and double sorted by FACS. The purity of the sorted αβ $CD8^+$ T cells was ≥ 99.8%. A mixture of 5×10^5 wt Thy1.1 and 5×10^5 Thy1.2 $\beta7^{-/-}$ (1:1 ratio) or 1×10^6 wt and 2×10^5 $\beta7^{-/-}$ (1:5 ratio) $CD8^+$ T cells were injected into chronically RV-infected Rag-2 mice. Three adoptively transferred Rag-2 recipient mice were sacrificed at each time point (days 7, 14, and 30 following the adoptive transfer). Intraepithelial lymphocytes (IELs), mesenteric lymph nodes (MLNs), and spleen cells were purified individually from each recipient Rag-2 mouse and were stained with anti-CD8 CyChrome, anti-Thy1.1 allophycocyanin (APC) and anti-Thy1.2 PE purchased from PharMingen. IEL, MLNs, and spleen cells were purified from unmanipulated Rag-2 mice (lacking B and T lymphocytes), stained with the same antibodies, and used as negative controls. The cells were analyzed using flow cytometry.

To compare the anti-rotaviral activity of $CD8^+$ T cells generated by oral versus subcutaneous immunizations, separate groups of wt mice were immunized orally or subcutaneously as described above. Spleen cell–suspensions from immunized wt mice were enriched for $CD8^+$ T cells by column purification, and were stained with anti-CD8 FITC, anti-$\alpha_4\beta_7$ PE, and biotinylated anti-CD44, purchased from PharMingen. The cells were washed and streptavidin-Red613 (Life Technologies Inc., Gaithersburg, Maryland, USA) was added to stain biotin-tagged cells. Subsequently, three-color cell sorting was performed using modified FACS-star with filters for FITC detection (530/30), for PE detection (585/42), and for Red 613 detection (630/22). The sorted cells (purity 99.5 ± 0.2%) were resuspended in sterile saline solution and 10,000 $CD44^+$, $\alpha_4\beta_7^{hi}$, and 30,000 $CD44^+$, $\alpha_4\beta_7^{low}$ $CD8^+$ T cells were injected intraperitoneally into chronically infected Rag-2 mice. Three days following adoptive transfer, control recipient mice were sacrificed and lymphocytes from spleen, MLNs, or intestinal intraepithelial lymphocytes (iIELs) were subjected to flow cytometric analysis. We were not able to detect any residual lymphocyte staining with the anti-$\alpha_4\beta_7$ integrin or CD8 antibodies in any of the tissues tested (data not shown).

FITC labeling of splenocytes. Splenocytes from naive $\beta7^{-/-}$ or wt mice were labeled with FITC as previously described (20). Frozen stocks of FITC (Sigma-Aldrich Chemie GmbH, Deisenhofen, Germany) were diluted in 50% DMEM, 50% HBSS, and 2.5% FBS, pH 7.0 to a concentration of 38 μg/ml. Five to six million spleen cells were incubated for 20 minutes with 2 ml FITC (38 mg/ml) at 37°C. The labeled spleen cells were spun through 7 ml of FBS to remove the excess FITC and subsequently washed twice with HBSS. 2×10^7 FITC-labeled cells were injected intravenously into naive C57BL/6 recipients.

Isolation of lymphocyte populations. iIEL populations were isolated from the recipient Rag-2 mice as described previously (21). MLNs and spleens of the transferred immunodeficient Rag-2 mice were removed 30 days following the adoptive transfer. Single cell suspensions were prepared using a sterile cell strainer as described above.

In vivo depletion. Mice were depleted of $CD8^+$ T cells by administration of ascites containing rat anti-mouse CD8 mAb 2.43 as previously described (22). In brief, each mouse received 0.5 ml of ascitic fluid intraperitoneally 5, 4, and 3 days before RV infection; on the day of RV infection; and on days 3, 6, and 9 after infection. Depleted and nondepleted control mice were sacrificed at day 25 following the RV infection to detect $CD8^+$ T cells in the spleen, MLNs, and IELs by flow cytometry. All flow cytometry data were analyzed with the CELLQUEST program (Becton Dickinson Immunocytometry Systems) on a Macintosh computer (Apple Computer Inc., Cupertino, California, USA).

ELISPOT for RV-specific cytokine producing cells. The method used was described in detail previously (23). Splenocytes from subcutaneously or orally immunized animals were analyzed for IFN-γ spot-forming (SF) cells. Splenocytes were passed through a CD8 purification column and subsequently separated by FACS into $\alpha_4\beta_7^{hi}$ and $\alpha_4\beta_7^{low}$ populations. To generate cytokines, the purified $CD8^+$ T cells were stimulated with enriched dendritic cell (DC) populations obtained as described by Nair et al. (24). Splenocytes from naive 8- to 10-week-old female C57BL/6 mice were depleted of erythrocytes, and 3 ml of cells at concentration 1×10^7 per ml were layered over 2 ml of a metrizamide gradient (Nycomed Pharma A, Oslo, Norway; analytical grade,14.5 g added to 100 ml of PBS, pH 7.0). The cells were then centrifuged at 600 *g* for 10 minutes, and the cells at the interface were collected. The enriched DC populations were pulsed for 4 hours with cesium-purified, psoralen-treated, and UV-inactivated RRV (50 μg/1×10^6 DCs) and used as stimulators. The responder FACS purified $CD8^+$ $\alpha_4\beta_7^{hi}$ or $\alpha_4\beta_7^{low}$ T cell populations and the stimulators were mixed at stimulator/responder ratios of 50:1, 25:1, and 12.5:1 in 200 μl of 10% FBS DMEM and plated into coated and blocked ELISPOT plates. The ELISPOT plates were precoated with anti–IFN-γ) (PharMingen) at a concentration of 2 μg/ml in 100 μl of sterile carbonate buffer and incubated at 4°C overnight. Subsequently the plates were blocked with DMEM 10% FBS for 1 hour at 37°C. After 72 hours of incubation of the effector and stimulator cells (in a vibration-free incubator), the ELISPOT plates were washed and biotinylated anti–IFN-γ antibody (PharMingen) diluted 1:10000 in PBS 1% FBS was added to the plate. After 1 hour of incubation at 37°C the plates were washed, streptavidin-conjugated alkaline phosphatase (diluted 1:2000) was added, and the plates were incubated at 37°C for an additional 1 hour. Subsequently the plates were developed using nitro blue tetrazolium (NBT) and 5-bromo-4-chloro-3-inodolyl phosphate (BCIP) (Sigma Immuno-Chemicals) substrates and the spots were counted 24 hours later using a dissecting microscope.

Quantification of anti-RV $CD8^+$ T cells with VP-7 specific tetramers. The RV-specific MHC I ($H\text{-}2K^b$) restricted tetramer was constructed as previously described (25). In

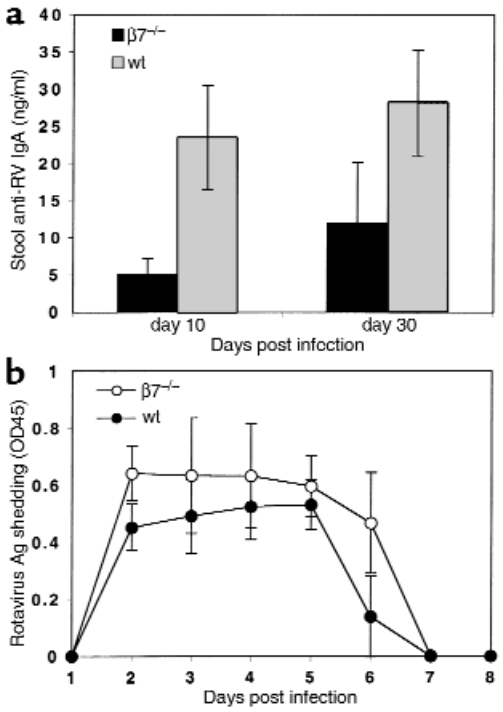

Figure 1
Anti-RV IgA response and virus shedding in the stool of $\beta7^{-/-}$ and wt mice following oral infection with RV. Data were combined from six mice in each group. (**a**) Level of intestinal anti-RV IgA in $\beta7^{-/-}$ or wt mice at days 10 and 30 after oral RV infection. Data were determined by ELISA (presented as ng/ml). (**b**) Stool RV Ag shedding from $\beta7^{-/-}$ (open circles) and wt (filled circles) mice following oral infection with mRV. (Total Ag shedding was not significantly different between the two groups of mice.)

brief, the recombinant MHC molecule was folded in the presence of mouse β2-microglobulin and a rotaviral VP7 peptide epitope (IVYRFLLV) (previously shown to contain the dominant H-2K^b restricted CD8 T-cell epitope in C57BL/6 mice [ref. 26]) to form a peptide-MHC complex, following the procedure of Garboczi et al. (27). After biotinylation using the enzyme BirA, the complex was mixed with APC-conjugated streptavidin (PharMingen) at molar ratios of 4:1 to form the peptide MHC tetramer.

For four-color FACS analysis, a mixture containing RV-specific tetramer conjugated to APC (2 μg), anti-CD8 Cy-Chrome (0.5 μg), FITC-labeled antibodies to CD13, CD4, and CD19 (0.5 μg), and anti-$\alpha_4\beta_7$ PE (0.5 μg) was added to 1×10^6 spleen cells. After 30 minutes of incubation at room temperature in the dark, the cells were washed with FACS buffer (PBS 2.5% BCS, 0.1% Na Azide), fixed in 1% paraformaldehyde, and analyzed on a FACScalibur flow cytometer.

Immunofluorescence. Seven-micron cryosections from ileum of selected mice were fixed for 8 minutes in acetone at 4°C. Sections were then blocked with 10% normal hamster serum (Jackson ImmunoResearch Laboratories Inc., West Grove, Pennsylvania, USA) for 30 minutes. Slides were incubated for 5 hours at room temperature with biotinylated hamster anti-mouse CD3ε at 1.33 μg/ml (PharMingen). After washing three times for 5 minutes each, streptavidin-conjugated Texas Red (Jackson ImmunoResearch Laboratories Inc.) was added at 1:300 and incubated for 1 hour in the dark at room temperature. Slides were washed three times for 5 minutes each, coverslipped with vectashield (Vector Laboratories, Burlingame, California, USA) and analyzed with a scanning confocal microscope. Negative controls included omission of the primary antibody or replacement of the primary antibody with an isotype-matched hamster IgG_{2a} antibody.

Results

$\beta7^{-/-}$ mice clear primary RV infection with the same efficiency as wt mice. Following oral infection with mRV, the level of RV shedding and anti-RV antibody secretion in the stool was determined from fecal samples collected from $\beta7^{-/-}$ or wt (C57BL/6) mice. $\beta7^{-/-}$ mice developed significantly less intestinal anti-RV IgA compared to wt mice following oral RV infection (Figure 1a). Despite diminished intestinal humoral immunity, $\beta7^{-/-}$ mice were able to resolve primary RV infection at the same rate as wt animals (Figure 1b).

To determine whether resolution of primary RV infection in $\beta7^{-/-}$ mice was CD8$^+$ T-cell dependent, $\beta7^{-/-}$ mice were depleted of CD8$^+$ T cells using mAb's (see Methods). Antibody-treated mice exhibited a substantial reduction in the number of CD8$^+$ T-cells in the iIEL compartment, confirming successful depletion (Figure 2a). Accordingly, CD8$^+$ T cell–depleted mice exhibited significant prolongation of RV shedding compared with nondepleted $\beta7^{-/-}$ mice (Figure 2b). The duration of rotaviral Ag shedding was similar to that in CD8$^+$ T cell–depleted wt mice (data not shown, and ref. 28). These results indicate that, as in wt mice, CD8$^+$ T cells are involved in the timely resolution of primary RV infection in $\beta7^{-/-}$ mice.

Immune CD8$^+$ T cells resolve RV infection when transferred from $\beta7^{-/-}$ mice into chronically infected Rag-2 deficient mice. We used an adoptive transfer approach to evaluate the influence of $\alpha_4\beta_7$ expression on the effector function of CD8$^+$ T cells. As previously described (29), Rag-2 mice become chronically infected when orally inoculated with mRV (Figure 3a). These mice were used as recipients for CD8$^+$ splenic T cells derived from $\beta7^{-/-}$ or wt mice that had previously cleared RV. The ability of adoptively transferred CD8$^+$ T cells to resolve chronic RV infection was monitored by measuring daily RV shedding in stools of recipient Rag-2 mice. Adoptive transfer of 5×10^3 immune $\beta7^{-/-}$ or wt CD8$^+$ T cells into infected Rag-2 mice failed to clear RV infection (Figure 3, b and c); clearance was variable when 5×10^4 immune CD8$^+$ T cells were transferred (Figure 3, d and e), but all Rag-2 recipient mice given 5×10^5 $\beta7^{-/-}$ or wt CD8$^+$ T cells resolved infection (Figure 3, f and g). No difference in the duration of shedding was observed between Rag-2 mice given $\beta7^{-/-}$ or wt immune CD8$^+$ T cells at each cell number injected. These findings indicate a quantitative threshold for RV clearance by immune CD8$^+$ T cells that was independent of $\alpha_4\beta_7$ expression.

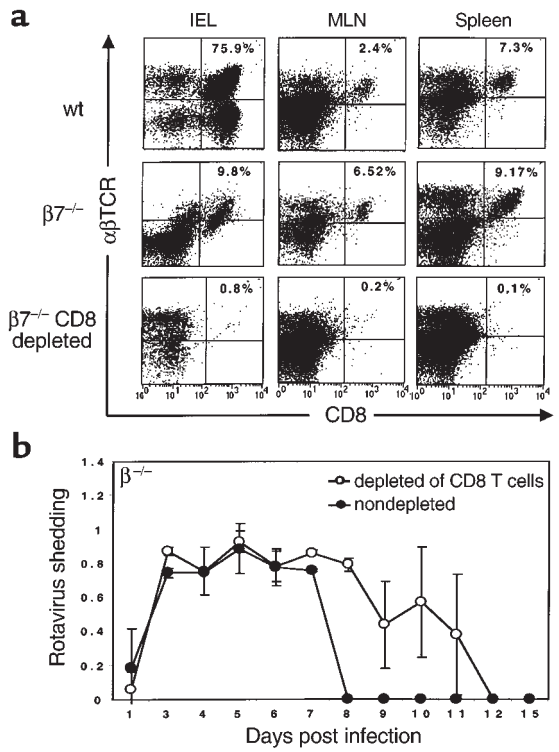

Figure 2
RV shedding of β7$^{-/-}$ mice depleted of CD8$^+$ T cells with mAb. The effect of anti-CD8 mAb treatment on CD8$^+$ T-cell populations and rotaviral shedding is shown. (**a**) Flow cytometry data indicating CD8$^+$ αβ T-cell populations in different tissues of β7$^{-/-}$ and wt mice that were treated or untreated with anti-CD8 mAb. β7$^{-/-}$ mice were depleted of CD8$^+$ T cells and subsequently infected with RV as described in Methods. At day 25 from the beginning of the experiment, the mice were sacrificed and IEL, MLNs, and spleen cells were purified, stained with anti-CD8 and anti-TCRαβ antibodies, and analyzed by FACS. (**b**) Stool samples were collected daily following RV infection, and the levels of RV Ag were determined by ELISA. SD is based on four animals per group (the figure represents one out of two experiments performed with similar results).

Using flow cytometry, CD19$^+$ (B cells) and CD4$^+$ cells were not detected in the Rag-2 mice following transfer with immune CD8$^+$ T cells, confirming that the donor cells were not contaminated (data not shown). The absence of B cell contamination was further supported by the observation that anti-RV IgA remained undetectable in the stool of Rag-2 mice 30 days after CD8$^+$ T-cell transfer (data not shown). Hence we were unable to show a quantitative or qualitative difference in the effector function of β7$^{-/-}$ versus wt CD8$^+$ T cells.

$\alpha_4\beta_7^{-/-}$ CD8$^+$ T cells can migrate to the IEL compartment of chronically infected Rag-2 mice. To determine whether the $\alpha_4\beta_7$ deficient CD8$^+$ T cells migrated into the intestinal epithelium, the percentage of CD8$^+$ TCRαβ$^+$ cells in the iIEL compartment of Rag-2 mice was evaluated at day 30 following adoptive transfer (Figure 4). For comparison, the percentage of TCRαβ$^+$ CD8$^+$ cells in the spleen and MLNs was also determined since lymphocyte migration to these organs is not dependent on $\alpha_4\beta_7$ integrin expression.

As anticipated, wt mice possessed CD8$^+$ T cells in all three compartments (iIEL, MLNs, and spleen) while the treated Rag-2 mice had virtually no detectable TCRαβ$^+$ cells in any of these compartments. In contrast, on day 30 following RV clearance, CD8$^+$ αβ $^+$ donor T cells were detected in iIEL, spleen, and MLNs of Rag-2 mice regardless of whether they expressed $\alpha_4\beta_7$ integrin (Figure 4).

A somewhat lower percentage of lymphocytes was recovered from the iIEL compartment of chronically infected Rag-2 mice reconstituted with purified CD8$^+$ TCRαβ$^+$ cells from β7$^{-/-}$ mice (14.7%) than from wt mice (34.0%) (Figure 4). The absolute number of cells recovered from iIEL of chronically infected Rag-2 mice at day 30 following adoptive transfer of β7$^{-/-}$ or wt CD8$^+$ T cells was similar (in the range of $2–6 \times 10^6$ cells per mouse). When the percentages of CD8$^+$ T cells in iIELs from six animals per group were compared (wt versus β7$^{-/-}$) the differences were not statistically significant ($P > 0.05$) (using Student *t* test) (see Figure 7d).

$\alpha_4\beta_7^{-/-}$(Thy1.2) CD8$^+$ T cells can migrate to the intestine when $\alpha_4\beta_7$ positive wt (Thy1.1) immune CD8$^+$ T cells are present. To test whether migration into the intestinal mucosa of $\alpha_4\beta_7$ integrin–deficient CD8$^+$ T cells occurred independently of $\alpha_4\beta_7$ ligand binding, we examined the competition for iIEL entry between $\alpha_4\beta_7$-deficient and wt CD8$^+$ T cells. We used wt (Thy1.1) and β7$^{-/-}$ (Thy1.2) mice as donors. Thirty days following RV infection of wt (Th1.1) or β7$^{-/-}$ (Th1.2) mice splenic CD8$^+$ T cells were affinity-purified and double FACS sorted (purity ≥ 99.8%). A mixture of 5×10^5 β7$^{-/-}$ and 5×10^5 wt CD8$^+$ T cells was adoptively transferred into the same Rag-2 recipients. The recipients were sacrificed at 14 days following adoptive transfer (when viral infection had cleared from the intestine) and the percentages of β7$^{-/-}$ or wt CD8$^+$ T cells in the iIEL were determined using flow cytometry. In all adoptively transferred Rag-2 mice we observed distinct populations of β7$^{-/-}$ and wt CD8$^+$ T cells in both iIEL and MLN compartments (Figure 5, a and b). The percentage of β7$^{-/-}$ T cells in the iIEL was ten times lower than wt CD8$^+$ T cells (Figure 5a). When five times more wt than β7$^{-/-}$ T cells were transferred, we were still able to detect $\alpha_4\beta_7$ deficient CD8$^+$ T cells in the iIEL (percentages were from 15- to 20-fold lower than wt T cells, data not shown). These findings suggest that $\alpha_4\beta_7$-deficient T cells were able to migrate to iIEL even in the presence of competing wt CD8$^+$ T cells, consistent with the notion that they were trafficking into the iIEL via an alternative recognition signal.

Histological analysis of intestinal tissues from RV-challenged Rag-2 mice in the presence or absence of adoptively transferred β7$^{-/-}$ or wt CD8$^+$ T cells. Immunohistological examination of intestinal tissue from adoptively transferred Rag-2 mice was performed to determine the location of adoptively transferred lymphocytes. RV-infected Rag-2 mice, reconstituted with immune CD8$^+$ T cells from β7$^{-/-}$ or wt mice, were sacrificed at day 30 after adoptive transfer, and sec-

Figure 3
Fecal rotaviral Ag shedding in Rag-2 mice chronically infected with RV following adoptive transfer of varying numbers of immune $\beta7^{-/-}$ or wt $CD8^+$ splenic T cells. Donor mice were immunized orally as described in Methods, and spleen cells from these donor mice were harvested 30 days after immunization. (**a**) Ag shedding in RV-infected Rag-2 mice not transferred with cells. (**b** and **c**) RV Ag shedding of Rag-2 mice transferred with 5×10^3 $CD8^+$ T cells. (**d** and **e**) RV Ag shedding of Rag-2 mice transferred with 5×10^4 $CD8^+$ T cells. (**f** and **g**) RV Ag shedding of Rag-2 mice transferred with 5×10^5 $CD8^+$ T cells. Asterisks represent RV Ag shedding in chronically infected Rag-2 mice that did not receive immune cells (**a**). Open circles represent RV shedding in Rag-2 mice adoptively transferred with $\beta7^{-/-}$ $CD8^+$ T cells (**b**, **d**, and **f**). Filled circles represent RV shedding in Rag-2 mice adoptively transferred with wt $CD8^+$ T cells (panels **c**, **e**, and **g**).

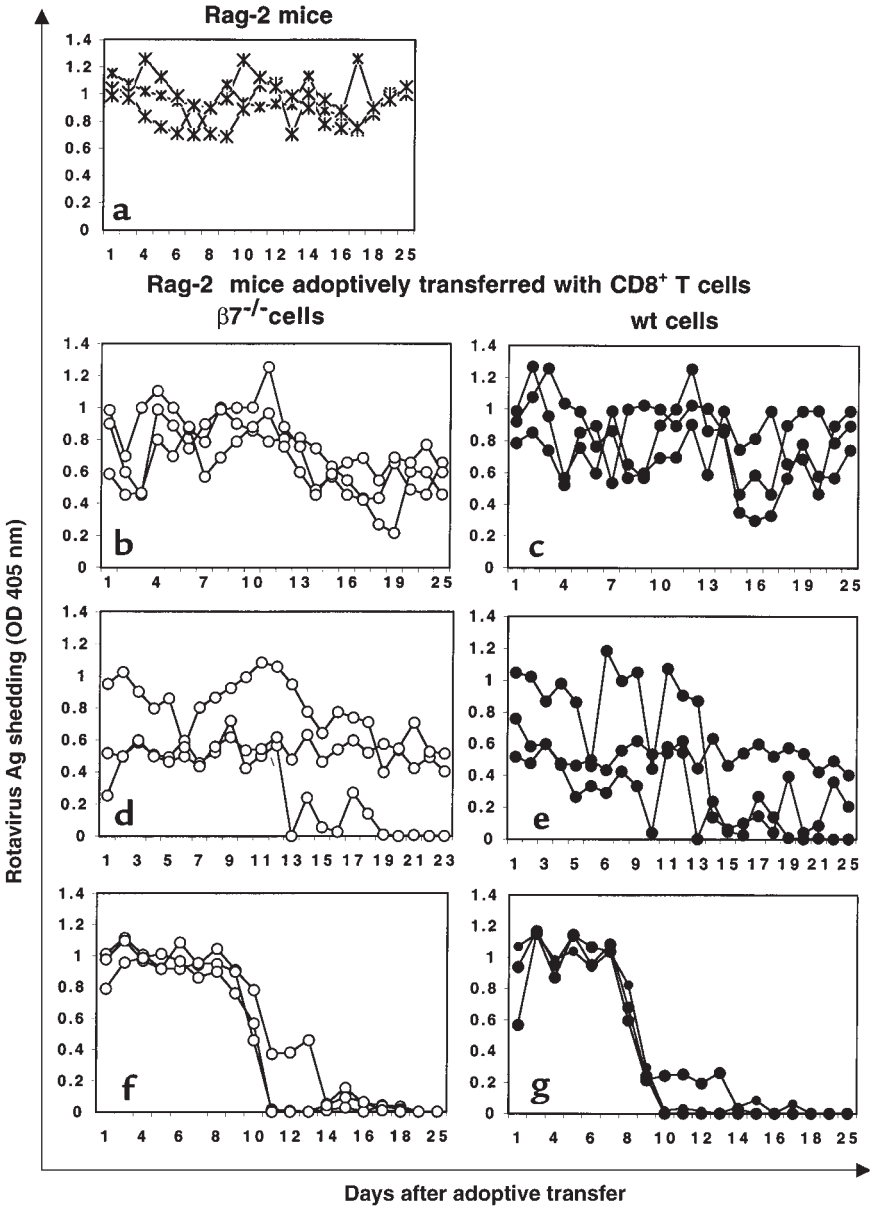

tions of ileum were used for histological analysis. Intestinal sections from wt and untreated Rag-2 mice served as controls (Figure 6, a and b). $CD3^+$ cells were detected in the iIEL compartment of wt mice (Figure 6a) but, as expected, not in mice that were Rag-2 (Figure 6b). On the other hand, Rag-2 mice that received wt or $\beta7^{-/-}$ $CD8^+$ T cells demonstrated $CD3^+$ cells in both IEL and lamina propria (LP) compartments of the intestine (Figure 6, c and d).

The time of reconstitution of the IEL compartment with $\beta7^{-/-}$ or wt $CD8^+$ T cells correlates with resolution of RV shedding. To follow the migration of the transferred $\beta7^{-/-}$ or wt $CD8^+$ T cells in chronically infected Rag-2 mice, recipients were sacrificed at different time points after cell transfer and IEL, MLNs, and spleen cells were analyzed by flow cytometry (Figure 7). At 3 hours (Figure 7a) and 3 days (data not shown) after transfer, the highest percentage of transferred $CD8^+$ $\alpha\beta^+$ T cells was found in the spleen (and blood, data not shown). By 7 days after transfer, the highest percentage of transferred immune cells was detected in the MLNs, but none were detected in the iIEL (Figure 7b). Correspondingly, rotaviral replication in the intestine continued during the same period (Figure 3, f and g). By day14, $\beta7^{-/-}$ and wt $CD8^+$ $\alpha\beta^+$ T cells were detected in the IEL of the respective recipient Rag-2 mice (Figure 7, c and d). Correspondingly, the mice resolved rotaviral infection. Thus, the presence of $CD8^+$ T cells in the IEL compartment correlated temporarily with rotaviral clearance independently of $\alpha_4\beta_7$ expression.

The iIEL compartment remained populated with $CD8^+$ T cells through 30 days following cell transfer. The percentage of $\beta7^{-/-}$ $CD8^+$ T cells in the iIEL of recipient Rag-2 mice remained lower relative to the wt

CD8+ T cells. Differences in percentages of CD8+ T cells in iIEL between groups (each composed of six animals) were not statistically significant ($P > 0.05$), however (Figure 7, c and d).

Oral immunization with live mRV generates RV-specific CD8+ T cells in the $\alpha_4\beta_7^{hi}$ memory cell population whereas subcutaneous administration of inactivated RRV generates anti-RV CD8+ effectors with both $\alpha_4\beta_7^{low}$ and $\alpha_4\beta_7^{hi}$ phenotypes. The experiments described above demonstrate that $\alpha_4\beta_7$ expression is not a requirement for CD8+ T cell–mediated immunity against RV in the intestinal mucosa. However, in an earlier study we showed that $\alpha_4\beta_7^{hi}$ CD8+ splenic T cells from orally infected wt mice resolved chronic RV infection more efficiently in Rag-2 mice than $\alpha_4\beta_7^{low}$ cells (8). Given our new findings with $\beta7^{-/-}$ mice, we postulated that the reason we had not observed effective antirotaviral immunity with $\alpha_4\beta_7^{low}$ spleen cells (see Figure 10a and ref. 8) might be due to the presence of fewer RV-specific CD8+ T cells in $\alpha_4\beta_7^{low}$ versus $\alpha_4\beta_7^{hi}$ subsets following oral immunization rather than a low level of intestinal homing integrin expression in the $\alpha_4\beta_7^{low}$ population. Therefore we quantified the number of RV-specific CD8+ T cells in the splenic populations of donor mice. These were the cells used for adoptive transfer into RV infected Rag-2 mice. We specifically determined the frequency of anti-RV splenic CD8+ T cells in $\alpha_4\beta_7^{hi}$ and $\alpha_4\beta_7^{low}$ populations following oral versus subcutaneous immunization with RV.

Wt mice were immunized orally with live mRV or subcutaneously with inactivated RRV in CFA and IFA (as described in Methods). Systemic immunization was employed with the hope that RV immune CD8+ T cells might be induced efficiently in the $\alpha_4\beta_7^{low}$ population. For systemic immunizations, inactivated RRV was used because this virus, in contrast to mRV, does not spread to the intestine when administered subcutaneously. To further eliminate this possibility, we chemically treated and UV-inactivated the RRV. Successful inactivation was confirmed by demonstrating lack of viral replication in the inactivated RRV preparations when cultured in vitro (data not shown).

Two approaches were adopted to determine the frequency of RV-specific CD8+ T cells in the immunized mice: ELISPOT assay and staining of Ag-specific CD8+ T cells using an MHC class I tetramer. Thirty days following immunization, we determined the frequency of IFN-γ SF CD8+ T cells (23) from systemically or orally immunized mice after in vitro restimulation. Oral immunization generated 26 IFN-γ SF CD8+ T cells/10^4 $\alpha_4\beta_7^{hi}$ CD8+ T cells, whereas only two IFN-γ SF CD8+ T cells were detected in the $\alpha_4\beta_7^{low}$ population (Figure 8). On the other hand, systemic administration with inactivated RV generated IFN-γ–producing cells at a frequency of 4 and 10 SF cells/1×10^4 CD8+ T cells in the $\alpha_4\beta_7^{hi}$ and $\alpha_4\beta_7^{low}$ populations, respectively (Figure 8).

The high ratio of $\alpha_4\beta_7^{hi}$ to $\alpha_4\beta_7^{low}$ RV-specific CD8+ T cells (26:2) was confirmed using class I restricted tetramer staining (Figure 9). A higher percentage of RV-specific CD8+ T cells was found in the $\alpha_4\beta_7^{hi}$ fraction of orally immunized animals (0.16%), consistent with our previous ELISPOT results, whereas very few RV-specific CD8+ T cells were detected in the $\alpha_4\beta_7^{low}$ fraction (0.03%). In contrast, both assays demonstrated that subcutaneous immunization generated RV-specific CD8+ T cells in both $\alpha_4\beta_7^{hi}$ and $\alpha_4\beta_7^{low}$ populations (0.23% and 0.22% by tetramer analysis [Figure 8] and 4 ± 2 and 10 ± 4 by ELISPOT analysis [Figure 9]).

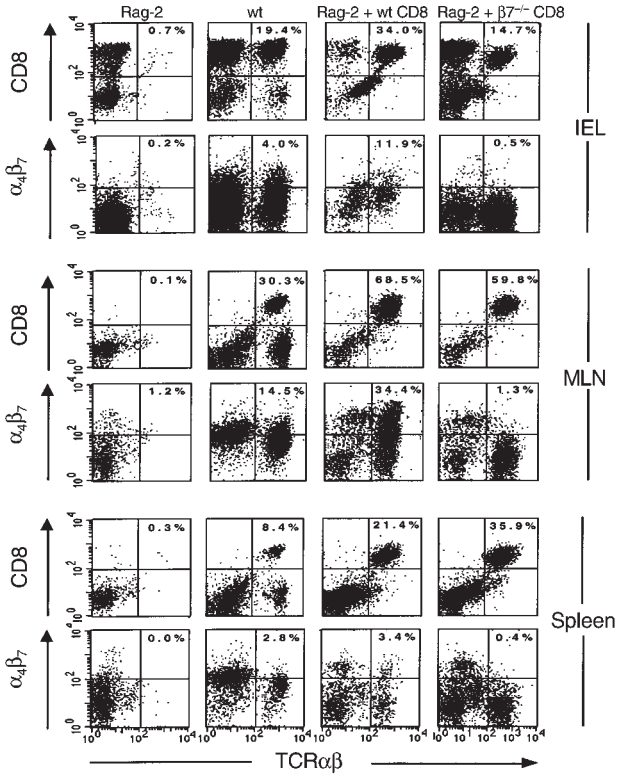

Figure 4
Flow cytometric analysis of IEL, MLNs, and spleen cells from RV-infected Rag-2 mice 30 days after transfer of 5×10^5 $\beta7^{-/-}$ or wt CD8+ T cells. Cells from Rag-2 and wt (C57BL/6) mice served as controls. Cells were double-stained with anti-CD8 FITC and anti-TCRαβ PE or with anti-CD8 FITC and anti-$\alpha_4\beta_7$ PE as described in Methods. Percentage of cells in the quadrant of interest is indicated.

$\alpha_4\beta_7^{low}$ CD8+ T cells from subcutaneously immunized wt donor mice can eliminate RV infection from chronically infected Rag-2 recipients. We next tested the in vivo ability of $\alpha_4\beta_7^{hi}$ and $\alpha_4\beta_7^{low}$ CD8+ T cells purified from subcutaneously versus orally immunized mice to clear RV when transferred into chronically infected Rag-2 mice. Initially we confirmed our previous studies (8) demonstrating that 10,000 purified $\alpha_4\beta_7^{hi}$ CD8+ T cells from orally immunized wt mice efficiently resolved chronic RV infection when transferred into Rag-2 mice (Figure 10c), whereas 30,000 $\alpha_4\beta_7^{low}$ CD8+ T cells (threefold more) from the same donors could not resolve infection (Figure 10a). In contrast, 30,000 $\alpha_4\beta_7^{low}$ CD8+ T cells transferred from subcutaneously immunized wt mice efficiently resolved RV infection in Rag-2 mice (Figure 10b). Although both

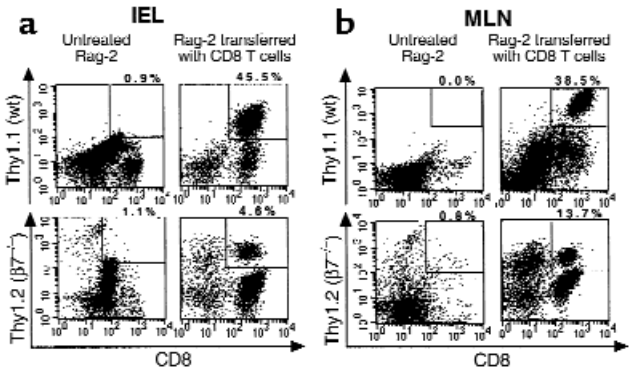

Figure 5
FACS analyses of IEL and MLN cells purified from RV-infected Rag-2 mice at day 14 following adoptive transfer of 5×10^5 $\beta7^{-/-}$ (Thy1.2) and 5×10^5 wt (Thy1.2) $CD8^+$ T cells. IEL and MLN cells from untreated Rag-2 mice served as controls. (**a**) Percentage of wt (Thy1.1) or $\beta7^{-/-}$ (Thy1.2) $CD8^+$ T cells in the IEL. (**b**) Percentage of wt (Thy1.1) or $\beta7^{-/-}$ (Thy 1.2) $CD8^+$ T cells in the MLNs.

$\alpha_4\beta_7^{low}$ and $\alpha_4\beta_7^{hi}$ cell populations underwent homeostatic expansion in the recipient Rag-2 mice (similar number of cells were recovered from the spleen MLNs and iIEL compartments, data not shown), only $\alpha_4\beta_7^{hi}$ $CD8^+$T cells were able to resolve RV infection (Figure 10b). These results demonstrate that subcutaneous RV immunization generated protective anti-RV $CD8^+$ T cells in the $\alpha_4\beta_7^{low}$ population.

Discussion

This study demonstrates that $\alpha_4\beta_7$ integrin expression on memory $CD8^+$ T cells is not essential for those cells to migrate to the gut and resolve RV infection. Our results suggest the existence of a β7-independent mechanism of $CD8^+$ T cell migration to and/or retention in the intestine. This alternative mechanism appears sufficient to direct and/or retain $CD8^+$ TCR$\alpha\beta^+$ cells to intestinal effector sites in the absence of both $\alpha_4\beta_7$ and $\alpha_E\beta_7$ integrin expression. We also provide evidence that oral immunization with live RV generates Ag-specific $CD8^+$ T cells almost exclusively in the $\alpha_4\beta_7^{hi}$ population, whereas subcutaneous RV administration induces a more divided $CD8^+$ T cell immune response in both $\alpha_4\beta_7^{hi}$ and $\alpha_4\beta_7^{low}$ cell fractions.

Previous studies have specifically correlated intestinal lymphocyte homing with expression of the $\alpha_4\beta_7$ integrin. In vitro and short-term in vivo experiments have shown the importance of $\alpha_4\beta_7$ in lymphocyte homing to Peyer's patches (PP) and intestinal LP (3, 5–7, 30, 31). In vivo experiments demonstrated more efficient homing of $\alpha_4\beta_7^{hi}$ versus $\alpha_4\beta_7^{low}$ memory T cells to PP (7). A recent report using gene targeting to disrupt β_7 integrins led to drastically impaired formation of the gut associated lymphoid tissue, due to the inability of β_7 integrin deficient lymphocytes to efficiently migrate through the high endothelial venules into this compartment (9).

Here, using β7-deficient animals and intestinal RV infection, we assessed the role played by $\alpha_4\beta_7$ integrin expression in promoting $CD8^+$ T cell effector function in the gut. Because in mice, as well as in humans, RV replication is localized to the villus tips of the intestinal epithelium, the RV mouse model is particularly helpful in identifying key components of mucosal immune effector function.

Consistent with the observation that $\beta7^{-/-}$ mice have a defective gut inductive immune system (9), $\beta7^{-/-}$ mice orally infected with RV generated lower levels of intestinal anti-RV IgA compared to wt controls (Figure 1). Despite diminished antiviral humoral responses, $\beta7^{-/-}$ mice cleared RV from the intestine at the same time as wt animals (day 7 following infection), suggesting the efficient involvement of class I mediated T-cell immunity. $\beta7^{-/-}$ mice depleted of $CD8^+$ T cells were able to clear RV days 10 after infection just like $CD8^+$ T cell–depleted wt mice (28). The prolongation of RV shedding in $CD8^+$ T cell–depleted versus nondepleted $\beta7^{-/-}$ mice indicates that $\beta7^{-/-}$ $CD8^+$ T cells contribute to the timely clearance of RV during primary infection despite the absence of $\alpha_4\beta_7$ integrin expression. Although fewer $CD8^+$ T cells are found in the iIEL of $\beta7^{-/-}$ compared with wt mice (Figure 2a), these cells appear to be sufficient to hasten the elimination of virus from the intestinal epithelium during primary infection (Figure 2b). It is possible that during primary infection $\beta7^{-/-}$ $CD8^+$ T cells already present in the intestine become primed locally and subsequently clear RV infection.

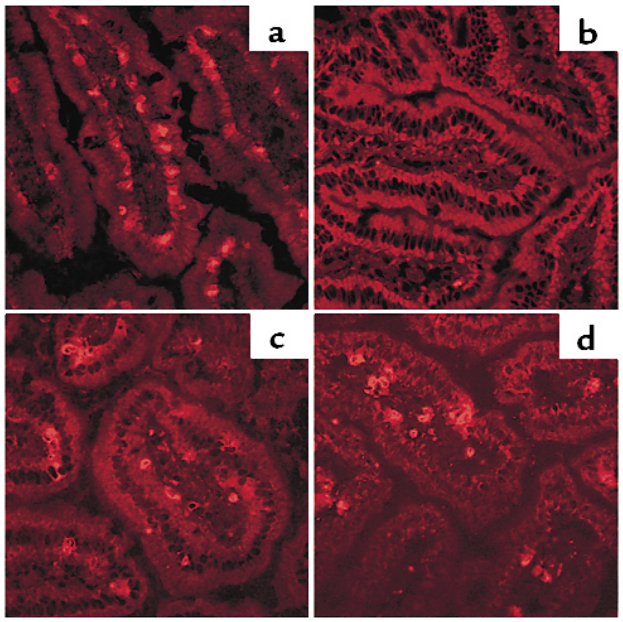

Figure 6
Immunohistological analyses of intestinal tissue sections obtained from the ilea of uninfected wt mice, uninfected Rag-2 mice, and chronically infected Rag-2 mice transferred with 5×10^5 $CD8^+$ T cells from RV-immune wt or $\beta7^{-/-}$ mice. The samples were stained with biotinylated anti-mouse CD3 followed by streptavidin-conjugated Texas red and were analyzed using confocal microscopy. (**a**) wt mouse (uninfected). (**b**) Rag-2 untreated mouse (uninfected). (**c**) Chronically infected Rag-2 mouse transferred with 5×10^5 wt $CD8^+$ T cells. (**d**) Chronically infected Rag-2 mouse transferred with 5×10^5 $\beta7^{-/-}$ $CD8^+$ T cells.

Figure 7
Percentage of CD8$^+$ TCR$\alpha\beta^+$ cells in IELs, MLNs, and spleens of mice transferred with $\beta7^{-/-}$ or wt CD8$^+$ T cells at indicated times after transfer. (**a**) Percentage of CD8$^+$ TCR$\alpha\beta^+$ FITC-labeled cells. Splenocytes from nonimmune $\beta7^{-/-}$ or wt mice were labeled in vitro with FITC and 10^7 cells were injected intravenously into C57BL/6 recipient mice. Three hours following injection of the labeled cells, recipient mice were sacrificed and percentages of CD8$^+$ T cells in the indicated tissues were determined by FACS. (**b**, **c**, and **d**) Chronically infected Rag-2 mice were adoptively transferred with 5×10^5 CD8$^+$ T cells from RV immune $\beta7^{-/-}$ or wt mice. Seven (**b**), 14 (**c**), and 30 (**d**) days after transfer, recipient mice were sacrificed and cells from IEL, MLNs, and spleen were analyzed by FACS. Each group consisted of six animals. Differences in percentages of CD8$^+$ T cells between groups (each comprising six animals) were not statistically significant using standard *t* test ($P > 0.05$). Note that the scales in **a** and **b** are different because fewer CD8$^+$ T cells were detected at 3 hours than at 7 days following adoptive transfer.

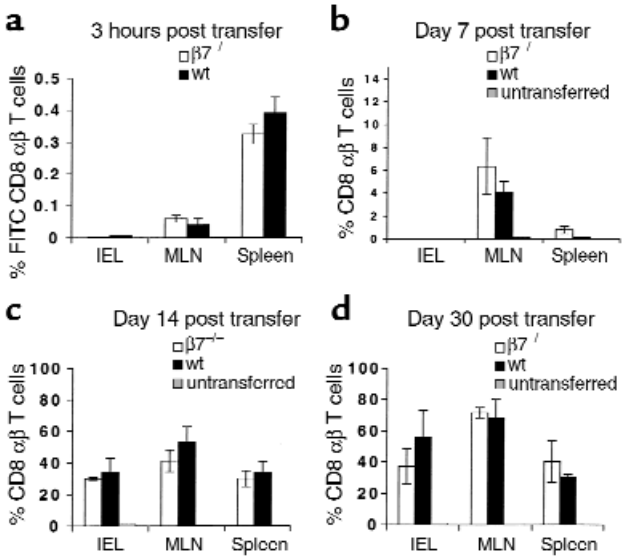

To directly evaluate the anti-RV function of CD8$^+$ T cells lacking $\alpha_4\beta_7$ and $\alpha_E\beta_7$, we used an adoptive transfer mouse model. We used $\beta7^{-/-}$ mice as a source of immune CD8$^+$ T cells and compared their anti-RV effector function with that of wt CD8$^+$ T cells after passive transfer. We injected log order differences (5×10^3, 5×10^4, and 5×10^5) of $\beta7^{-/-}$ or wt CD8$^+$ TCR$\alpha\beta^+$ cells into chronically infected Rag-2 mice and compared the kinetics and efficiency of viral clearance. We could not detect a difference either in the level or duration of RV Ag shedding between chronically infected Rag-2 mice injected with $\beta7^{-/-}$ or wt CD8$^+$ T cells (Figure 3). Although a small difference in efficiency could have been missed in our analysis, $\beta7^{-/-}$ CD8$^+$ T cells did not appear to be substantially less efficient than wt cells in mediating antiviral function in the intestine.

We purified iIELs of the recipient Rag-2 mice at different time points following CD8$^+$ T cell transfer and analyzed them by flow cytometry to determine whether the injected $\beta7^{-/-}$ CD8$^+$ T cells were actually migrating to the site of viral replication. CD8$^+$ TCR$\alpha\beta^+$ T cells were found in the iIEL compartment of the recipient Rag-2 mice at time points synchronous with, but not before, virus elimination. At 3 hours, 3 days, and 7 days after cell transfer, CD8$^+$ T cells were found in both spleen and MLNs, but, if present in iIEL compartment, their frequency was too low to resolve RV infection or to be detected by flow cytometry (Figure 7). Recovery of CD8$^+$ T cells from the iIEL compartment correlated temporally with viral clearance from the intestine. $\beta7^{-/-}$ CD8$^+$ T cells could still migrate to the intestine even when adoptively transferred simultaneously with wt CD8$^+$ T cells into the same recipients (Figure 5). This observation indicated that $\alpha_4\beta_7$-deficient CD8$^+$ T cells were not blocked by wt CD8$^+$ T cells migrating into the intestine and further supports the existence of an $\alpha_4\beta_7$-independent mechanism of CD8$^+$ T cell migration into the gut epithelium.

Our findings are consistent with a recent report using class I restricted ovalbumin (OVA) transgenic mice and systemic infection with recombinant Vesicular Stomatitis Virus expressing OVA (rVSV OVA) to study the role of the $\alpha_4\beta_7$ and $\alpha_E\beta_7$ integrins in intestinal homing (13). This study also identified some residual ability of $\beta7^{-/-}$ cells to migrate to the gut. It was unclear, however, whether the residual ability of $\beta7^{-/-}$ memory cells to migrate to effector sites would be sufficient to exert an immune effector function during intestinal infection. In the present study, using a common gut pathogen, we

Figure 8
IFN-γ ELISPOT assay. RV-responsive cells are mainly in $\alpha_4\beta_7^{hi}$ population of orally but not subcutaneously immunized mice. Splenocytes from C57BL/6 mice immunized orally or subcutaneously with RV were enriched for CD8$^+$ T cells using affinity column purification. Subsequently, the cells were FACS-sorted into $\alpha_4\beta_7^{hi}$- or $\alpha_4\beta_7^{low}$-expressing CD44$^+$ (memory) $\alpha\beta$ TCR CD8$^+$ T cells. The sorted cells were restimulated in vitro for 72 hours, and the frequency of IFN-γ SFCs was determined by ELISPOT. The figure represents one out of three experiments performed with similar results. Five mice were used per group in each experiment. The SD is based on three replicates per group.

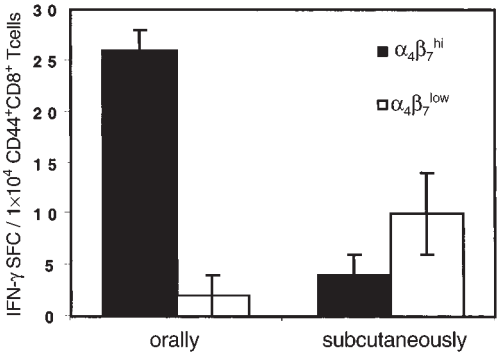

Figure 9
Tetramer staining for RV-specific CD8+ T cells. RV-responsive cells are mainly in $\alpha_4\beta_7^{hi}$ population of orally but not subcutaneously immunized mice. Wt mice (C57BL/6) were immunized twice at a 15-day interval either subcutaneously or orally with RV as described. Thirty days following the last immunization, the splenocytes from immune mice were stained with anti-CD8 CyChrome; anti-CD19, anti-CD13, and anti-CD4 FITC; anti-$\alpha_4\beta_7$ PE; and class I tetramer APC. Small lymphocytes were negatively gated on FITC-stained cells and positively gated on anti-CD8 CyChrome–stained cells. The gated cells were analyzed for $\alpha_4\beta_7$ PE expression and tetramer-APC binding. Splenocytes from nonimmunized mice were stained simultaneously and were used as negative control. As negative control we also used APC-conjugated class I tetramer specific for irrelevant Ag. The gates for $\alpha_4\beta_7$-negative cells and $\alpha_4\beta_7$-expressing cells were set using splenocytes from $\beta7^{-/-}$ mice. The data represent one out of three experiments performed with similar results. Three mice per group were used in each experiment.

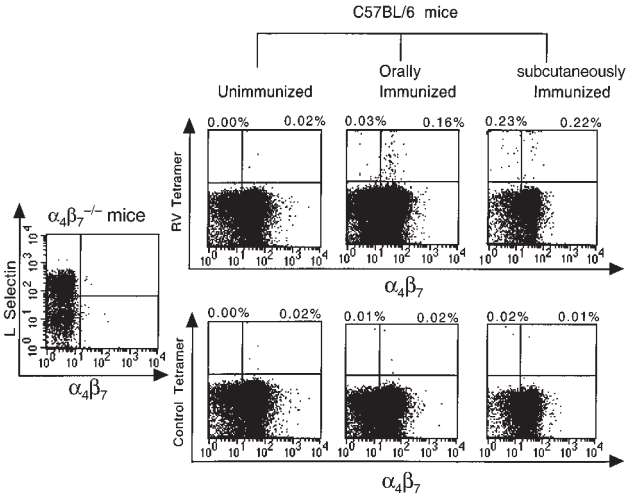

demonstrated that $\beta7^{-/-}$ CD8+ T cells, when compared with wt CD8+ T cells, are able to mediate anti-RV activity in the intestine with similar efficiency during primary infection and adoptive transfer (Figures 1, 2, and 3).

The successful function of $\beta7^{-/-}$ CD8+ T cells in the gut, as demonstrated here, provides further evidence for redundancy within the immune system and points to the existence of an alternative mechanism of CD8+ T cell trafficking to and/or retention at intestinal effector sites. Molecules other than β7 seem likely to be involved in directing CD8+ T cells to RV-infected intestinal epithelium. For example, β2 integrins have been suggested as candidates for directing intestinal CD8+ T cells (32), a possibility we are currently investigating. This would be consistent with the multistep model of lymphocyte homing in which $\alpha_4\beta_7$ integrins initiate gut homing and are thought to have serial but partially overlapping functions in vascular endothelial recognition (33).

Recently it has been demonstrated that intestinal RV infection in young mice can induce expression of various chemokines by intestinal epithelial cells (34). A CC chemokine, thymus expressed chemokine (TECK), and its receptor CCR9 (predominantly expressed on memory $\alpha_4\beta_7^+$, CD4+, and CD8+ T cells) are selectively expressed in the small intestine, implying a potential role in intestinal immunity (35). It is possible that RV-induced chemokines could additionally activate and recruit $\beta7^{-/-}$ CD8+ T cells in the intestine, facilitating their local expansion. Future studies will be designed to explore this possibility.

In contrast to the ability of $\beta7^{-/-}$ and wt CD8+ T cells to resolve RV infection when injected into chronically infected Rag-2 mice, $\alpha_4\beta_7^{low}$ CD8+ T cells purified

Figure 10
Wt mice (C57BL/6) were immunized twice at a 15-day interval either subcutaneously or orally with RV as described. Thirty days following the last immunization, the memory CD8+ T cells from the spleen were separated by FACS into $\alpha_4\beta_7^{hi}$ or $\alpha_4\beta_7^{low}$ fractions and subsequently injected into chronically infected Rag-2 mice. The data represent one of two experiments performed with similar results. (**a**) Stool Ag shedding of RV-infected Rag-2 mice adoptively transferred with 30,000 $\alpha_4\beta_7^{low}$ memory CD8+ T cells purified from mice orally immunized with live RV. (**b**) Virus shedding of RV-infected Rag-2 mice adoptively transferred with 30,000 $\alpha_4\beta_7^{low}$ memory CD8+ T cells purified from mice systemically immunized with inactivated RV. (**c**) Stool Ag shedding of RV-infected Rag-2 mice adoptively transferred with 10,000 $\alpha_4\beta_7^{hi}$ memory CD8+ T cells purified from mice orally immunized with live RV. (**d**) Stool Ag shedding of RV-infected Rag-2 mice adoptively transferred with 10,000 $\alpha_4\beta_7^{hi}$ memory CD8+ T cells purified from mice systemically immunized with inactivated RV. Circles indicate RV shedding of Rag-2 mice transferred with CD8+ T cells from orally immunized donors. Squares indicate RV shedding of Rag-2 mice transferred with CD8+ T cells from systemically primed donors. Filled symbols indicate Ag shedding of Rag-2 mice adoptively transferred with $\alpha_4\beta_7^{hi}$ CD8+ T cells. Open symbols indicate Ag shedding of Rag-2 mice adoptively transferred with $\alpha_4\beta_7^{low}$ CD8+ T cells.

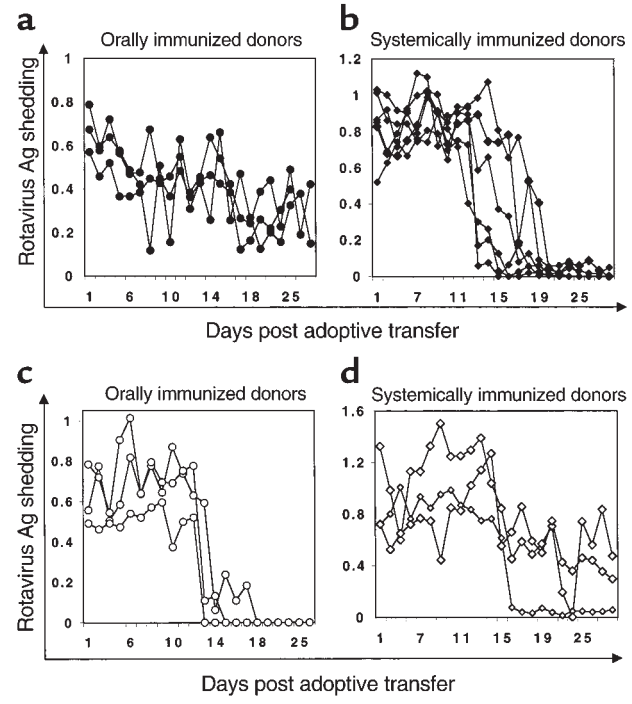

from orally immunized immunocompetent mice were much less efficient than $\alpha_4\beta_7^{hi}$ $CD8^+$ T cells at clearing RV infection (8). Based on our results with $\beta7^{-/-}$ mice, we hypothesized that this difference might not reflect a requirement for $\alpha_4\beta_7$ expression on memory $CD8^+$ T cells, but rather resulted from selective enrichment of RV-specific memory $CD8^+$ T cells in the $\alpha_4\beta_7^{hi}$ subset after oral immunization. In this study we provided evidence that the $\alpha_4\beta_7^{low}$ population of $CD8^+$ T cells purified from orally immunized mice was not protective when transferred into RV-infected Rag-2 mice because it contained very few RV-specific immune $CD8^+$ T cells (Figures 8 and 9). We were able to increase the frequency of RV-specific $CD8^+$ T cells in the $\alpha_4\beta_7^{low}$ population by subcutaneous immunization with inactivated RV. Using this immunization route, we observed that 30,000 purified memory $\alpha_4\beta_7^{low}$ $CD8^+$ $TCR\alpha\beta^+$ T cells were able to resolve RV infection when injected into chronically infected Rag-2 mice, whereas the opposite was observed after adoptive transfer of $\alpha_4\beta_7^{hi}$ $CD8^+$ $TCR\alpha\beta^+$ T cells from orally immunized animals.

To determine the frequency of RV-specific $CD8^+$ T cells in the $\alpha_4\beta_7^{hi}$ and $\alpha_4\beta_7^{low}$ populations of orally and systemically immunized animals, we used two assays: RV (VP7) specific class I restricted tetramer staining and Ag-specific IFN-γ ELISPOT assay. Both approaches demonstrated that oral immunization generated anti-RV $CD8^+$ T cell immunity almost exclusively in the $\alpha_4\beta_7^{hi}$ population. A substantial increase in the frequency of RV-specific $CD8^+$ T cells in the $\alpha_4\beta_7^{low}$ fraction was achieved when inactivated RRV was injected systemically. Hence the principle reason $\alpha_4\beta_7^{low}$ $CD8^+$ T cells from orally immunized mice fail to eradicate chronic RV infections is that they contain few, if any, RV-specific memory cells. These data are consistent with our previous study in humans demonstrating that anti RV $CD4^+$ T cell immunity also resides primarily in the $\alpha_4\beta_7^{hi}$ population (36). In addition, we have shown that oral immunization of mice with live RV generates RV-specific Ig producing cells (measured by RV-specific ELISPOT) primarily in the $\alpha_4\beta_7^{hi}$ B cell populations (37).

It is widely assumed that systemic immunity is best induced by parenteral immunization, whereas mucosal responses are generated as a result of Ag exposure at mucosal surfaces. Our data support this notion. However we also demonstrate that systemic (subcutaneous), but not oral immunization can prime protective anti-$CD8^+$ T cell immunity in $\alpha_4\beta_7^{low}$, as well as $\alpha_4\beta_7^{hi}$, populations. Hence, induction of immune $\alpha_4\beta_7^{hi}$ and $\alpha_4\beta_7^{low}$ $CD8^+$ T cells does occur after systemic immunization. On the other hand, oral immunization strongly favors the induction of $\alpha_4\beta_7^{hi}$ immune $CD8^+$ T cells with little immunity residing in the $\alpha_4\beta_7^{low}$ population. Surprisingly, local RV immune effector functions can be mediated by either fraction of $CD8^+$ T cells. Whether this is true for other $CD8^+$ T cell–mediated local anti-microbial effects remains to be determined. It will also be important to determine if B cells with low or absent $\alpha_4\beta_7$ expression can mediate anti-RV effects, since the ability to induce efficient humoral mucosal effector function following systemic immunization would widen the possibility for the design of vaccines against mucosal pathogens.

Acknowledgments

We thank Stewart L. Cooper for constructive editorial comments and helpful suggestions. We thank Sally Morefield for secretarial assistance. This work was supported by NIH grant R37AI21362, a Veterans Administration Merit Review grant to H.B. Greenberg, and NIH training grant 5 T32 AI07328-12 to N.A. Kuklin.

1. Ahmed, R., and Gray, D. 1996. Immunological memory and protective immunity: understanding their relation. *Science*. **272**:54–60.
2. Murphy, B.R. 1996. Immunization against virus disease. In *Virology*. Volume 1. B.N. Fields, editor. Lippincott-Raven Publishers. Philadelphia, Pennsylvania, USA. 15–59.
3. Butcher, E.C., Williams, M., Youngman, K., Rott, L., and Briskin, M. 1999. Lymphocyte trafficking and regional immunity. *Adv. Immunol.* **72**:209–253.
4. Rose, J., Franco, M., and Greenberg, H. 1998. The immunology of rotavirus infection in the mouse. *Adv. Virus Res*. **51**:203–235.
5. Holzmann, B., McIntyre, B.W., and Weissman, I.L. 1989. Identification of a murine Peyer's patch: specific lymphocyte homing receptor as an integrin molecule with an alpha chain homologous to human VLA-4 alpha. *Cell*. **56**:37–46.
6. Hamann, A., Andrew, D.P., Jablonski, W.D., Holzmann, B., and Butcher, E.C. 1994. Role of alpha 4-integrins in lymphocyte homing to mucosal tissues in vivo. *J. Immunol*. **152**:3282–3293.
7. Williams, M.B., and Butcher, E.C. 1997. Homing of naive and memory T lymphocyte subsets to Peyer's patches, lymph nodes, and spleen. *J. Immunol*. **159**:1746–1752.
8. Rose, J.R., Williams, M.B., Rott, L.S., Butcher, E.C., and Greenberg, H.B. 1998. Expression of the mucosal homing receptor alpha4beta7 correlates with the ability of CD8+ memory T cells to clear rotavirus infection. *J. Virol*. **72**:726–730.
9. Wagner, N., et al. 1996. Critical role for beta7 integrins in formation of the gut-associated lymphoid tissue. *Nature*. **382**:366–370.
10. Steeber, D.A., et al. 1998. Efficient lymphocyte migration across high endothelial venules of mouse Peyer's patches requires overlapping expression of L-selectin and beta7 integrin. *J. Immunol*. **161**:6638–6647.
11. Wagner, N., et al. 1998. L-selectin and beta7 integrin synergistically mediate lymphocyte migration to mesenteric lymph nodes. *Eur. J. Immunol*. **28**:3832–3839.
12. Kunkel, E.J., et al. 1998. The roles of L-selectin, beta 7 integrins, and P-selectin in leukocyte rolling and adhesion in high endothelial venules of Peyer's patches. *J. Immunol*. **161**:2449–2456.
13. Lefrancois, L., et al. 1999. The role of beta7 integrins in CD8 T cell trafficking during an antiviral immune response. *J. Exp. Med*. **189**:1631–1638.
14. Cepek, K.L., et al. 1994. Adhesion between epithelial cells and T lymphocytes mediated by E-cadherin and the alpha E beta 7 integrin. *Nature*. **372**:190–193.
15. Burns, J.W., et al. 1995. Analyses of homologous rotavirus infection in the mouse model. *Virology*. **207**:143–153.
16. Hoshino, Y., Wyatt, R.G., Greenberg, H.B., Flores, J., and Kapikian, A.Z. 1984. Serotypic similarity and diversity of rotaviruses of mammalian and avian origin as studied by plaque-reduction neutralization. *J. Infect. Dis*. **149**:694–702.
17. Groene, W.S., and Shaw, R.D. 1992. Psoralen preparation of antigenically intact noninfectious rotavirus particles. *J. Virol. Methods*. **38**:93–102.
18. Offit, P.A., Clark, H.F., and Plotkin, S.A. 1983. Response of mice to rotaviruses of bovine or primate origin assessed by radioimmunoassay, radioimmunoprecipitation, and plaque reduction neutralization. *Infect. Immun*. **42**:293–300.
19. Kuklin, N., Daheshia, M., Karem, K., Manickan, E., and Rouse, B.T. 1997. Induction of mucosal immunity against herpes simplex virus by plasmid DNA immunization. *J. Virol*. **71**:3138–3145.
20. Butcher, E.C., and Weissman, I.L. 1980. Direct fluorescent labeling of cells with fluorescein or rhodamine isothiocyanate. I. Technical aspects. *J. Immunol. Methods*. **37**:97–108.
21. Taguchi, T., et al. 1991. Novel function for intestinal intraepithelial

lymphocytes. Murine CD3+, gamma/delta TCR+ T cells produce IFN-gamma and IL-5. *J. Immunol.* **147**:3736–3744.
22. Franco, M.A., and Greenberg, H.B. 1995. Role of B cells and cytotoxic T lymphocytes in clearance of and immunity to rotavirus infection in mice. *J. Virol.* **69**:7800–7806.
23. Kuklin, N.A., Daheshia, M., Chun, S., and Rouse, B.T. 1998. Immunomodulation by mucosal gene transfer using TGF-beta DNA. *J. Clin. Invest.* **102**:438–444.
24. Nair, S., Zhou, F., Reddy, R., Huang, L., and Rouse, B.T. 1992. Soluble proteins delivered to dendritic cells via pH-sensitive liposomes induce primary cytotoxic T lymphocyte responses in vitro. *J. Exp. Med.* **175**:609–612.
25. Altman, J.D., et al. 1996. Phenotypic analysis of antigen-specific T lymphocytes [erratum 1998, **280**:1821]. *Science.* **274**:94–96.
26. Franco, M.A., et al. 1993. An immunodominant cytotoxic T cell epitope on the VP7 rotavirus protein overlaps the H2 signal peptide. *J. Gen. Virol.* **74**:2579–2586.
27. Garboczi, D.N., Hung, D.T., and Wiley, D.C. 1992. HLA-A2-peptide complexes: refolding and crystallization of molecules expressed in Escherichia coli and complexed with single antigenic peptides. *Proc. Natl. Acad. Sci. USA.* **89**:3429–3433.
28. Franco, M.A., Tin, C., and Greenberg, H.B. 1997. CD8+ T cells can mediate almost complete short-term and partial long-term immunity to rotavirus in mice. *J. Virol.* **71**:4165–4170.
29. Dharakul, T., Rott, L., and Greenberg, H.B. 1990. Recovery from chronic rotavirus infection in mice with severe combined immunodeficiency: virus clearance mediated by adoptive transfer of immune CD8+ T lymphocytes. *J. Virol.* **64**:4375–4382.
30. Bargatze, R.F., Jutila, M.A., and Butcher, E.C. 1995. Distinct roles of L-selectin and integrins alpha 4 beta 7 and LFA-1 in lymphocyte homing to Peyer's patch-HEV in situ: the multistep model confirmed and refined. *Immunity.* **3**:99–108.
31. Picarella, D., et al. 1997. Monoclonal antibodies specific for beta 7 integrin and mucosal addressin cell adhesion molecule-1 (MAdCAM-1) reduce inflammation in the colon of scid mice reconstituted with CD45RBhigh CD4+ T cells. *J. Immunol.* **158**:2099–2106.
32. Huleatt, J.W., and Lefrancois, L. 1996. Beta2 integrins and ICAM-1 are involved in establishment of the intestinal mucosal T cell compartment. *Immunity.* **5**:263–273.
33. Butcher, E.C., and Picker, L.J. 1996. Lymphocyte homing and homeostasis. *Science.* **272**:60–66.
34. Rollo, E.E., et al. 1999. The epithelial cell response to rotavirus infection. *J. Immunol.* **163**:4442–4452.
35. Zaballos, A., Gutierrez, J., Varona, R., Ardavin, C., and Marquez, G. 1999. Cutting edge: identification of the orphan chemokine receptor GPR-9-6 as CCR9, the receptor for the chemokine TECK. *J. Immunol.* **162**:5671–5675.
36. Rott, L.S., et al. 1997. Expression of mucosal homing receptor alpha4beta7 by circulating CD4+ cells with memory for intestinal rotavirus. *J. Clin. Invest.* **100**:1204–1208.
37. Williams, M.B., et al. 1998. The memory B cell subset responsible for the secretory IgA response and protective humoral immunity to rotavirus expresses the intestinal homing receptor, alpha4beta7. *J. Immunol.* **161**:4227–4235.